

# Thermodynamic properties of the trigonometric Rosen-Morse potential and applications to a quantum gas of mesons

Aram Bahroz Brzo\*

Physics Department (College of Education)

University of Sulaimani

New camp - Tasluja - Street 1- Zone 501 Sulaimania

As Sulaymaniyah, Iraq

David Alvarez-Castillo†

H.Niewodniczański Institute of Nuclear Physics, PAS

152 Ul. Radzikowskiego, Cracow, 31-342, Poland

Bogoliubov Laboratory of Theoretical Physics, JINR

6 Joliot-Curie St, Dubna 141980, Russian Federation

## Abstract

In this study we work out thermodynamic functions for a quantum gas of mesons described as color-electric charge dipoles. They refer to a particular parametrization of the trigonometric Rosen-Morse potential which allows to transform it to a perturbation of free quantum motion on the three-dimensional hyper-sphere,  $S^3$ , a manifold that can host only charge-neutral systems, the charge dipoles being the configuration of the minimal number of constituents. To the amount charge neutrality manifests itself as an important aspect of the color confinement in the theory of strong interaction, the Quantum Chromodynamics, we expect our findings to be of interest to the evaluation of temperature phenomena in the physics of hadrons and in particular in a quantum gas of color charge dipoles as are the mesons. The results are illustrated for  $f_0$  and  $J/\psi$  mesons.

keywords: Trigonometric Rosen Morse potential; partition function; mesons.

---

\*aram.brzo@univsul.edu.iq

†alvarez@theor.jinr.ru

# 1 Introduction

The study of the thermodynamical properties of any system begins with the calculation of its partition function. All thermodynamical or statistical properties can be obtained from the partition function since it contains all the information about the given system [1]. A basic example is provided by the ideal quantum gas of di-atomic molecules, whose properties have been extensively studied in atomic, and molecular physics [2, 3, 4, 5]. Di-atomic molecules are described by it as rigid or elastic dumbbells with the dumbbells tracing trajectories placed on a two-dimensional space of constant curvature, the sphere immersed into a flat three-dimensional space. At the level of the one-dimensional Schrödinger equation, the partition function relevant for this case is the one determined by the trigonometric Scarf potential. Besides the textbook example of the harmonic oscillator, partition functions are known for several exactly solvable potentials, among them the hyperbolic Scarf [6], and the trigonometric Pöschl-Teller potentials [7].

A specifically interesting case occurs when the embedding space is by itself of constant curvature and takes the shape of the three-dimensional sphere,  $S^3$ . Such a situation can happen in cases of eigenvalue problems based upon interactions which are most favorably solved in hyper-spherical coordinates. A prominent example for this is provided by the trigonometric Rosen-Morse potential [8] given by,

$$V_{tRM}^{(\bar{a},b)}(\chi) = \frac{\hbar^2 c^2}{2M c^2 R^2} \left[ \frac{\bar{a}(\bar{a}-1)}{\sin^2(\chi)} - 2b \cot(\chi) \right], \quad \chi = \frac{r}{R}, \quad (1)$$

$$0 \leq \chi \leq \pi,$$

where  $\chi$  is an angular variable,  $\bar{a}$  is a parameter,  $r$  is a relative distance in flat space,  $R$  is the matching length parameter. The one-dimensional Schrödinger equation with this potential,

$$\begin{aligned} \frac{\hbar^2 c^2}{2M c^2 R^2} \left( -\frac{d^2}{d\chi^2} + V_{tRM}^{(\bar{a},b)}(\chi) \right) U(\chi) = \\ \frac{\hbar^2 c^2}{2M c^2 R^2} \left[ (n + \bar{a})^2 - \frac{b^2}{(n + \bar{a})^2} \right] U(\chi), \end{aligned} \quad (2)$$

where  $n$  stands for the node number of the wave function, has a remarkable property. Namely, upon the variable and parameter changes according to [9],

$$\Phi(\chi) = \frac{U(\chi)}{\sin(\chi)}, \quad \bar{a} \rightarrow l + 1, \quad l = 0, 1, 2, \quad (3)$$

i.e. for integer values of the  $\bar{a}$  parameters, the equation (2) is transformed to

$$\begin{aligned} & \left( -\frac{\hbar^2 c^2}{2Mc^2} \Delta_{S^3}(\chi) - \frac{\hbar^2 c^2}{2Mc^2 R^2} 2b \cot(\chi) - \frac{\hbar^2 c^2}{2Mc^2 R^2} \right) \Phi(\chi) \\ &= \frac{\hbar^2 c^2}{2Mc^2 R^2} \left( k(k+2) - \frac{b^2}{(k+1)^2} \right) \Phi(\chi), \end{aligned} \quad (4)$$

with

$$\begin{aligned} -\Delta_{S^3}(\chi) &= \frac{-1}{R^2 \sin^2(\chi)} \frac{\partial}{\partial \chi} \sin^2(\chi) \frac{\partial}{\partial \chi} + \frac{l(l+1)}{R^2 \sin^2(\chi)} \\ &= \frac{1}{R^2} K^2(\chi), \quad k = n + l. \end{aligned} \quad (5)$$

Here  $\Delta_{S^3}(\chi)$  stands for the part of the Laplace-Beltrami operator on the three-dimensional hyper-sphere,  $S^3$ , of hyper-radius  $R$ , which depends on the second polar angle,  $\chi$ , while  $K^2(\chi)$  denotes the squared operator of the four-dimensional angular momentum in the same variable. The second polar angle parametrizing the hyper-sphere is now given by  $\chi = \widehat{r} / R$  where  $\widehat{r}$  is the arc of the particle's path read off from the North-pole. In this way, the  $\csc^2(\chi)$  part of the trigonometric Rosen-Morse potential becomes part of the kinetic energy operator on  $S^3$ , while the  $\cot(\chi)$  term acquires meaning of perturbation of the free quantum rotation on  $S^3$ . The case is quite interesting indeed, especially for the descriptions of systems of charged particles, be them of electric, or color-electric charges. The issue is that on closed manifolds the fields generated by single charges do not respect Gauss's theorem [10]. Closed manifolds are necessarily charge neutral and for the fundamental degrees of freedom there are charge-dipoles. From a technical point of view, this situation generalizes the case of the ideal gas of di-atomic molecules from two- to three dimensional surfaces of constant curvatures. Ideal Bose-Einstein and Fermi-Dirac quantum gases in any dimension have been extensively studied in the literature, see [11] as a Representative example.

Systems of this kind can appear in the electrodynamics of neutral fluids, for example, or in Quantum Chromodynamics (QCD), known to describe color-electric charge neutral systems. Such are for example all the so far observed mesons, which are composed by equal number of quarks and anti-quarks, and also all the detected baryons, composed by three quarks in a color-neutral state. The non-observability of color-electric charges in QCD is an important aspect of the fundamental phenomenon known under the name of "color confinement". It can easily be verified that the cotangent function solves the Laplace equation on  $S^3$  which establishes it as a harmonic function on this manifold, quite in parallel to the inverse distance potential in plane Euclidean space, a reason for which when

$$2b = \alpha Z, \quad \alpha = \frac{e^2}{4\pi\hbar c\epsilon_0}, \quad (6)$$

with  $\alpha$  being the fine-structure constant, and  $Z$  the electric charge, one refers to the cotangent function as to the “curved Coulomb” potential [12]. The remarkable point of the  $\cot(\chi)$  function is that on  $S^3$  it represents a potential generated by a charge-dipole configuration. Similarly, the parametrization of ref. [13]

$$2b = \alpha_s N_c, \quad (7)$$

where  $\alpha_s$  is the (running) strong coupling “constant”, and  $N_c$  the number of colors, appears suited for studies of the color neutrality of hadrons.

The version of  $V_{tRM}^{(l+1,b)}(\chi)$ , to be termed to as “color-dipole potential”, is suited for the description of multiplicities of states in a level which appear in charge neutral systems whose orbital angular momenta,  $l$  and node numbers,  $n$ , of the wave functions, are varying according to  $(l + n) = k$ , with  $k$  non negative integer. Such multiplicities are observed besides in the Hydrogen atom, also in a variety of meson spectra [13, 14].

In contrast, the general version,  $V_{tRM}^{(\bar{a},b)}(\chi)$  with real  $\bar{a}$  parameter, is suited for spectra in which both charge neutrality and state multiplicities are absent, as emerging in atomic and molecular systems. Both versions of the potential under discussion have been studied by the super-symmetric quantum mechanics and its exact solutions can be found among others in [15, 16]. Notice that a meson, in being constituted by a quark ( $q$ ) and an anti-quark ( $\bar{q}$ ), is a color dipole. A gluon, ( $g$ ), and an anti-gluon ( $\bar{g}$ ) represent another type of a color dipole, which also qualifies as a part of the internal structures of mesons. The potential in (4) possesses several essential traits of strong interactions. For example, at short distances it is Coulomb-like, while at larger distances it becomes “stringy” as it becomes dominated by a linear term, all properties well visible by its Taylor series expansion around origin (“North pole”),

$$-2b \cot \chi \approx -\frac{2b}{\chi} + \frac{4b}{3}\chi \dots, \quad \chi = \frac{\widehat{r}}{R}.$$

However, in contrast to the Coulomb- plus linear interaction (known in the literature as “Cornell potential”), the cotangent potential is of finite range and describes systems confined to finite hyper-spherical volumes. In effect, the potential under consideration provides a reasonable parametrization of the internal structure of mesons as  $(q\bar{q})$  color-dipoles moving in the field generated by  $(g\bar{g})$  color dipoles and justifies employment of the equations (4) and (7) in the description of the thermodynamical properties of mesonic quantum gases.

While the trigonometric Rosen-Morse potential in Eq. (1) has been frequently employed in spectroscopic studies, its thermodynamical properties are much less known [12, 17]. The reference [12] is exclusively devoted to the evaluation of the canonical partition function of the curved Coulomb potential alone, while in [17] the authors calculate the partition function of the potential in (1) for a fixed real value of the  $\bar{a}$  parameter, thus letting the summation run only over the node number,  $n$ . As explained above, the latter choice does not allow

the  $\csc^2(\chi)$  term to become part of the Laplace-Beltrami operator on  $S^3$ , a reason for which the aspects of state multiplicities and charge neutrality cannot be addressed. It is the goal of the current work to go beyond the aforementioned approaches and

- improve the expression for the canonical partition function reported in [12],
- work out the canonical and grand canonical partition functions relevant for color-electric charge neutral systems with state multiplicities in a level,
- work out various thermodynamic functions related to the aforementioned partition functions,
- study the influence of the finite volume of the space occupied by the quantum gas, fixed by the volume of the hyper-sphere.

More precisely, we shall calculate the partition functions for non-negative integer  $\bar{a}$  values, i.e. for  $\bar{a} = l + 1$ , with  $l = 0, 1, 2, \dots, k$ , extend the summation over  $(l + n) = k$ , and investigate the thermodynamic properties of the trigonometric Rosen-Morse potential on these grounds. All in all, the system under consideration is akin to one consisting of meson-meson molecules which behaves like a Bose-Einstein gas, which effectively conserves the total particle number. The standard definition of chemical potential follows, see [18]. A similar analysis for a similar bosonic system of a pion gas can be found in this work [19].

The text is structured as follows. The next section is devoted to the canonical partition function. In section 3 we calculate and plot all the thermodynamic functions following from this canonical partition function. In section 4 the grand canonical partition function is elaborated together with the corresponding pressure function. The results are illustrated on the examples of charmonium and  $f_0$  mesons. In this way we lay down the mathematical foundations for applications in particle physics of the color-dipole potential introduced above. The text closes with a brief summary of the results.

## 2 The canonical partition function $Z(\beta, b, R)$ of the color-dipole potential

To evaluate the canonical partition function for the potential in Eqs. (4)-(5), and (7) on  $S^3$ , the linear energy in units of MeV is read off from eq. (4) as,

$$E_k = \frac{\hbar^2 c^2}{2Mc^2 R^2} \left( (k+1)^2 - \frac{b^2}{(k+1)^2} \right), \quad (8)$$

where  $Mc^2$  is the reduced mass of the two-body system under consideration. Then the so called ‘‘rotational temperature’’ expresses as,  $T_{rot} = \frac{\hbar c}{R}$ . The kinetic energy contribution is represented in Eq. 8 by the  $(k+1)^2$  term while

the potential energy is contained in the  $b$  dependent term. As we will see next, the kinetic energy is indeed the most significant contribution to the partition function as the potential energy term decreases very rapidly beyond the first excited state.

The expression for the partition function which does not account for multiplicity of states in a level, here denoted by  $Z(\beta, b, R)$ , is given by.

$$Z(\beta, b, R) = \sum_{k=0}^{\infty} e^{-\beta(E_k - E_0)}, \quad (9)$$

where the thermodynamic  $\beta$  constant is defined as  $\beta = \frac{1}{K_B T}$ , with  $K_B$  standing for the Boltzmann constant. This function can be approximated according to,

$$\begin{aligned} Z(\beta, b, R) &\approx e^{\beta E_0} \int_0^{\infty} e^{-\beta x^2} dx \\ &= \frac{e^{\beta E_0} \sqrt{\pi} \operatorname{erfc}(\sqrt{\gamma\beta})}{2\sqrt{\gamma\beta}}, \quad \operatorname{Re}(\sqrt{\gamma\beta}) > 0, \end{aligned} \quad (10)$$

where

$$\gamma = \frac{\hbar^2 c^2}{2Mc^2 R^2}, \quad (11)$$

and  $\operatorname{erfc}(u)$  stands for the complementary error function [20].

In Fig. 1 we display the canonical partition function that ignores the multiplicities of the states in the levels. The definition of the partition function that accounts for states multiplicities, again denoted by  $Z(\beta, b, R)$  for the sake of not overloading the presentation with too much different notations, and concerning the potential under consideration, is standard [1] and given by,

$$Z(\beta, b, R) = \sum_{k=0}^{\infty} g_k e^{-\beta(E_k - E_0)}, \quad k = \ell + n, \quad g_k = (k+1)^2, \quad (12)$$

where the energy multiplicity in the levels is  $(k+1)^2$ -fold. Now, Eq. (12) can be evaluated as,

$$\begin{aligned} Z(\beta, b, R) &= e^{\beta E_0} \sum_{k=0}^{\infty} (k+1)^2 e^{-\beta E_k} \\ &\approx e^{\beta E_0} \int_0^{\infty} (x+1)^2 e^{-\beta E(x)} dx, \end{aligned} \quad (13)$$

where the discrete variable  $k$  has been approximated by a continuous one, denoted by  $x$ , the infinite sum has been approximated by integration, and the discrete energy  $E_k$  has become the function,  $E(x)$ . Figure 2 shows that due to the exponential factor in the expression for the partition function of Eq. (12) rapidly suppresses higher order contributions to the sum, with only a few terms

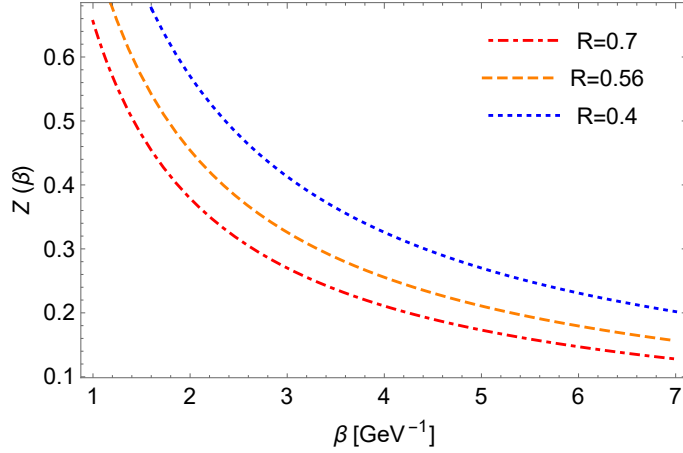


Figure 1: The canonical partition function in Eq. (10) as a function of  $\beta$ , with  $\beta$  varying from 1  $\text{GeV}^{-1}$  to 5  $\text{GeV}^{-1}$ . The parameters  $R$  and  $\alpha_s$  take the values 0.7, 0.56, 0.4 fm associated to  $0.66\pi, 0.2, 0.1$ , respectively.  $f_0(500)$  and charmonium values are denoted in red and orange colors.

needed to be very close to the above continuous approximation. Along this line, in Ref.[12], the partition function has been worked out for the case of  $b = \alpha Z/2$  and corresponds to the Hydrogen atom on  $S^3$ . With that, the partition function presents itself as,

$$Z(\beta, b, R) \approx e^{\beta E_0} \int_0^\infty (x+1)^2 e^{-a(x+1)^2 + \frac{p}{(x+1)^2}} dx, \quad (14)$$

where, we introduced the new notations of

$$a = \beta \gamma, \quad p = \beta \gamma b^2. \quad (15)$$

Now the integral can be evaluated by integration by parts yielding,

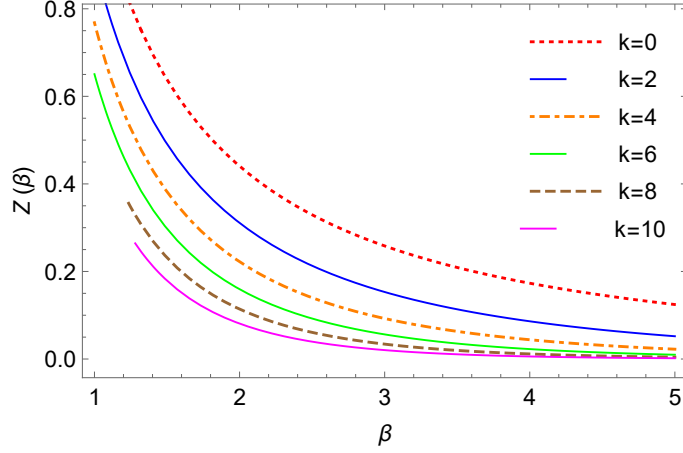


Figure 2: Partial contributions to the partition function from the  $k$ -term in Eq. (12). It can be seen that already for  $k = 10$  the contribution from this term is negligible, justifying the continuous approximation.

$$\begin{aligned}
& \int_0^\infty (x+1)^2 e^{-a(x+1)^2 + \frac{p}{(x+1)^2}} dx \\
&= \int_0^\infty (x+1)^2 e^{-a(x+1)^2} e^{\frac{p}{(x+1)^2}} dx \\
&= \frac{-1}{2a} \int_0^\infty (x+1) e^{\frac{p}{(x+1)^2}} d(e^{-a(x+1)^2}) \\
&= \frac{-1}{2a} (x+1) e^{\frac{p}{(x+1)^2}} e^{-a(x+1)^2} \Big|_0^\infty \\
&\quad + \frac{1}{2a} \int_0^\infty e^{-a(x+1)^2} d\left((x+1) e^{\frac{p}{(x+1)^2}}\right) \\
&= \frac{1}{2a} e^{p-a} + \frac{1}{2a} \int_0^\infty e^{-a(x+1)^2} e^{\frac{p}{(x+1)^2}} d(x+1) \\
&\quad + \frac{2p}{2a} \int_0^\infty e^{-a(x+1)^2 + \frac{p}{(x+1)^2}} d\left(\frac{1}{x+1}\right).
\end{aligned} \tag{16}$$

The argument of the exponential term under the integration sign can be represented as,

$$-a(x+1)^2 + \frac{p}{(x+1)^2} = -z^2 + 2i\sqrt{ap}, \quad z = \sqrt{a}(x+1) + i\frac{\sqrt{p}}{(x+1)} \tag{17}$$

where  $z$  is a complex number. Hence, substituting Eq. (16) and Eq. (17) into



Eq. (14), the partition function becomes,

$$\begin{aligned}
Z(\beta, b, R) &\approx \frac{1}{2a} + \frac{1}{2a} e^{\beta E_0} \int_0^\infty e^{-z^2 + 2i\sqrt{ap}} d(x+1) \\
&\quad + \frac{2p}{2a} e^{\beta E_0} \int_0^\infty e^{-z^2 + 2i\sqrt{ap}} d\left(\frac{1}{x+1}\right) \\
&\approx \frac{1}{2a} + \frac{1}{2a} e^{\beta E_0} \int_0^\infty e^{-z^2 + 2i\sqrt{ap}} d(x+1) \\
&\quad + \frac{1}{2a} e^{\beta E_0} \int_0^\infty e^{-z^2 + 2i\sqrt{ap}} d\left(\frac{2p}{x+1}\right),
\end{aligned}$$

equivalently,

$$Z(\beta, b, R) \approx \frac{1}{2a} + \frac{1}{2a} e^{\beta E_0} e^{2i\sqrt{ap}} \int_0^\infty e^{-z^2} d\left(x+1 + \frac{2p}{x+1}\right). \quad (18)$$

Then, with the aid of Eq. (17), we conclude on

$$\left(x+1 + \frac{2p}{x+1}\right) = \frac{1}{2} \left(\frac{1}{\sqrt{a}} - 2i\sqrt{p}\right) z + \frac{1}{2} \left(\frac{1}{\sqrt{a}} + 2i\sqrt{p}\right) z^*. \quad (19)$$

In effect, the partition function can be expressed in terms of the  $\operatorname{erfc}(u)$  function of complex argument,  $u \in \mathcal{C}_2$ . In so doing, Eq. (18) reduces to,

$$\begin{aligned}
Z(\beta, b, R) &\approx \frac{1}{2a} + \frac{1}{4a} e^{\beta E_0} \\
&\quad \times \left[ \left(\frac{1}{\sqrt{a}} - 2i\sqrt{p}\right) e^{2i\sqrt{ap}} \int_\Gamma e^{-z^2} dz \right. \\
&\quad \left. + \left(\frac{1}{\sqrt{a}} + 2i\sqrt{p}\right) e^{-2i\sqrt{ap}} \int_\Gamma e^{-(z^*)^2} dz^* \right],
\end{aligned} \quad (20)$$

where  $\Gamma$  is some path on the complex plane starting from  $u = 0$  and ending in

$u \rightarrow \infty$ . Thus, the partition function in Eq. (13) takes the following shape,

$$\begin{aligned}
Z(\beta, b, R) \approx & \frac{1}{2a} + \frac{1}{4a} e^{\beta E_0} \frac{1}{8a^{3/2}} \times \\
& (\sqrt{\pi} e^{-2\sqrt{a}\sqrt{-p}} (-\operatorname{erfc}(\frac{\sqrt{-p}}{x+1} - \sqrt{a}(x+1))) \\
& + e^{4\sqrt{a}\sqrt{-p}} (\operatorname{erfc}(\sqrt{a}(x+1) + \frac{\sqrt{-p}}{x+1} - 1) + 1) \\
& - 2\sqrt{\pi}\sqrt{a}\sqrt{-p} e^{-2\sqrt{a}\sqrt{-p^2}} (\operatorname{erfc}(\frac{\sqrt{-p}}{x+1} - \sqrt{a}(x+1))) \\
& e^{4\sqrt{a}\sqrt{-p}} (\operatorname{erfc}(\sqrt{a}(x+1) + \frac{\sqrt{-p}}{x+1} - 1) + 1) \\
& - 4\sqrt{a}(x+1) e^{-a(x+1)^2 + \frac{p}{(x+1)^2}} + c\dots).
\end{aligned} \tag{21}$$

Our expression for the canonical partition function in (21) differs from the one reported in [12] through the first term which in [12] takes the value of one, because there the integral in Eq. (16) has been evaluated for  $(x+1) \in [0, \infty]$ , while we evaluate it for  $x \in [0, \infty]$ , as it should be because the  $k$  parameter in (13) can not become negative. The additive  $1/(2a) = 1/(\beta b \gamma)$  correction to the canonical partition functions is important insofar as without it the partition function does not come out as a monotonous function of  $\beta$ .

Furthermore, as a further attempt to simplify the integration of Eq. (13), an approximate treatment can be suggested by using the Taylor series expansion [21]. Along this line, first the integration can be expanded around  $x = 0$ , according to,

$$\begin{aligned}
Z(\beta, b, R) = & \frac{1}{2a} + e^{\beta E_0} (e^{p-a} - 2k(e^{p-a}(a+p+1)) \\
& + k^2 e^{p-a} (2a^2 + a(4p-5)) \\
& + 2p^2 - p + 1) - \frac{2}{3} k^3 (e^{p-a} (2a^3 + a^2(6p-9)) \\
& + 6a(2p^2 - p + 1) + p^2(2p+3)) \\
& + \frac{1}{4} k^4 e^{p-a} (4a^4 + 4a^3(4p-7)) \\
& + 3a^2(8p^2 - 12p + 13) \\
& + 2a(8p^3 + 6p^2 + 3p - 3) + p^2(4p^2 + 20p + 15)) + O(x^5).
\end{aligned} \tag{22}$$

Back to the partition function in Eq. (14), we notice that with the increase of  $x$ , the contribution to the argument of the exponential provided by the term defined by the  $p$  parameter can be ignored compared to the term proportional to  $(x+1)^2$ . In addition, as visible from their definitions in (15) in combination

with (7), also the  $p$  parameter is significantly smaller than the  $a$  parameter, especially in the QCD regime of the asymptotic freedom where  $\alpha_s \rightarrow 0$ . For this case, the canonical partition function describes an ideal gas of color-electric dipoles, though the interaction has left its footprint through the presence of the  $p$  parameter in the  $e^{\beta E_0}$  factor with  $E_0 = (a-p)$ . Correspondingly, the canonical partition function under investigation becomes real and can be approximated as,

$$\begin{aligned}
Z(\beta, b, R) &\cong \frac{1}{2a} + 4 e^{-3\beta E_0} + \int_0^\infty (x+1)^2 e^{-\beta[(x+1)^2 E_0 - E_0]} dx \\
&\cong \frac{1}{2a} + 4 e^{-3\beta E_0} + e^{\beta E_0} \int_0^\infty (x+1)^2 e^{-\beta E_0 (x+1)^2} dx \\
&\cong \frac{1}{2a} + 4e^{-3\beta E_0} + \frac{\sqrt{\pi}}{4} \frac{1}{(E_0\beta)^{\frac{3}{2}}} e^{\beta E_0}.
\end{aligned} \tag{23}$$

Hereafter, if not said otherwise, we will consider the thermodynamic functions at fixed  $R$  value, and employ Eq. (23). In what follows we suppress the  $R$  and  $b$  arguments in  $Z(\beta, b, R)$  for the sake of simplifying notations, and focus on the dependence of the partition function on  $\beta$  alone, just writing  $Z(\beta)$ .

Now, the moment of inertia,  $I$ , is related to rotational temperature as,

$$\frac{\hbar^2 c^2}{2I} = K_B T_{rot}, \quad T_{rot} = \frac{\hbar c}{R}. \tag{24}$$

with

$$I = M c^2 R^2. \tag{25}$$

In addition, the classical energy  $E$  is related to the rotational temperature as,

$$E = K_B T_{rot}. \tag{26}$$

The Figure 3 represents the canonical partition function in (23) which accounts for the multiplicities. Notice the monotonous fall off of the function with  $\beta$ , a behavior ensured by the correct additive  $1/(2a)$  contribution to (23). In contrast, in [12], one encounters in place of  $1/(2a)$  the 1 constant, instead, in which case the partition functions is not monotonous. Comparison of Figs. 1 and 3 shows that as expected, the partition function accounting for the state multiplicities takes significantly larger values relative to the one which ignores them. Similar is the effect of the decreasing volume but it is notably smaller in size.

Both figures show that the partition functions corresponding to different volumes converge with  $R \rightarrow \infty$ , a tendency better pronounced by Fig. 2. The partition functions shown in Figs. 1, and 3 are both smooth functions of  $\beta$  and compare in shape with a similar result reported in Ref. [17], where the authors employed the trigonometric Rosen-Morse potential in the flat space

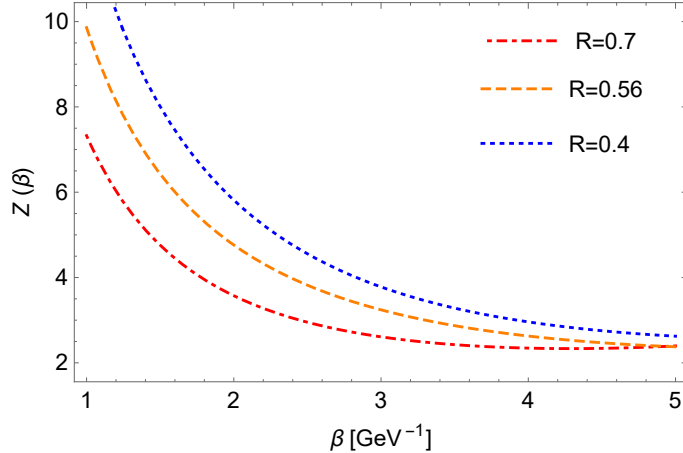


Figure 3: The partition function which accounts for multiplicities in Eq. (23) as a function of  $\beta$ , with  $\beta$  varying from 15  $\text{GeV}^{-1}$  to 5  $\text{GeV}^{-1}$ . The parameters  $R$  and  $\alpha_s$  take the values 0.7, 0.56, 0.4 fm associated to  $0.66\pi$ , 0.2, 0.1, respectively.  $f_0(500)$  and charmonium values are denoted in red and orange colors.

Schrödinger equation. Similar is the behavior of the partition functions of diatomic molecules [22], and of the harmonic-oscillator plus inverse-squared distance potential [23] as well of Pösch-Teller-type potentials [24]. Therefore, our choice of integer values for the  $\bar{a}$  parameter in the potential in Eq. (1), which was required by the  $S^3$  geometry that ensured the desired charge neutrality, does not alter the general behavior of the partition function with the change of  $\beta$ .

### 3 Thermodynamic properties following from the canonical partition function

This section is devoted to the elaboration of the thermodynamic functions following from the canonical partition function worked out in the previous section. According to [1], the main thermodynamic functions such as the internal energy ( $U(\beta)$ ), the energy fluctuation  $\langle (\Delta U(\beta))^2 \rangle$ , and the heat capacity ( $C(\beta)$ ) can be found from the canonical partition function  $Z(\beta)$  in Eq. (23) as,

$$\langle U(\beta) \rangle = \frac{-\partial \ln(Z(\beta))}{\partial \beta} = \frac{A}{B}, \quad (27)$$

amounting to,

$$\begin{aligned}
A &= 12E_0 e^{-3\beta E_0} - \frac{\sqrt{\pi}}{4} \left( \frac{E_0 e^{\beta E_0}}{(\beta E_0)^{\frac{3}{2}}} \right) \\
&+ \frac{3\sqrt{\pi}}{8} \left( \frac{E_0 e^{\beta E_0}}{(\beta E_0)^{\frac{5}{2}}} \right) + \left( \frac{1}{2\gamma\beta^2} \right), \\
B &= \frac{1}{2\gamma\beta} + 4 e^{-3\beta E_0} + \frac{\sqrt{\pi}}{4} \frac{1}{(E_0\beta)^{\frac{3}{2}}} e^{\beta E_0}. \quad (28)
\end{aligned}$$

Furthermore, the variation of the energy (or "energy fluctuation") is calculated

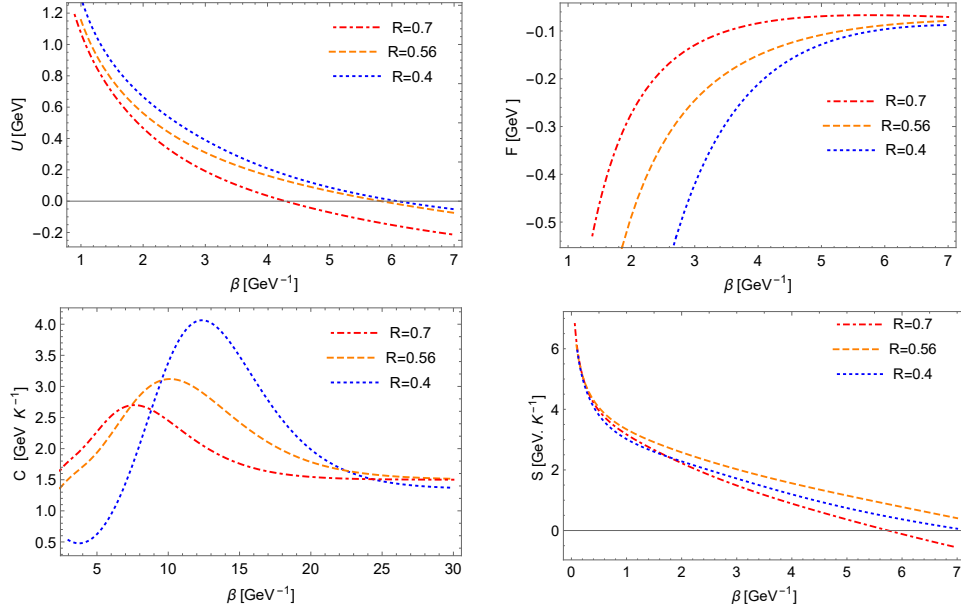


Figure 4: Thermodynamic quantities derived from  $Z(\beta, b, R)$ . Top: Internal energy  $U$  as derived in Eq. (27) and Helmholtz free energy  $F$  as derived in Eq.(31). Bottom: Heat capacity  $C$  as derived in Eq. (30) and entropy  $S$  as derived in Eq. (33). The parameters  $R$  and  $\alpha_s$  take the values 0.7, 0.56, 0.4 fm associated to  $0.66\pi$ , 0.2, 0.1, respectively.  $f_0(500)$  and charmonium values are denoted in red and orange colors.

as,

$$\begin{aligned}
\langle (\Delta U(\beta))^2 \rangle &= \frac{-\partial \langle U(\beta) \rangle}{\partial \beta} = \frac{\partial^2 \ln(Z(\beta))}{\partial \beta^2} \\
&= -\left( \frac{A}{B} \right)^2 + \frac{D}{B}, \quad (29)
\end{aligned}$$

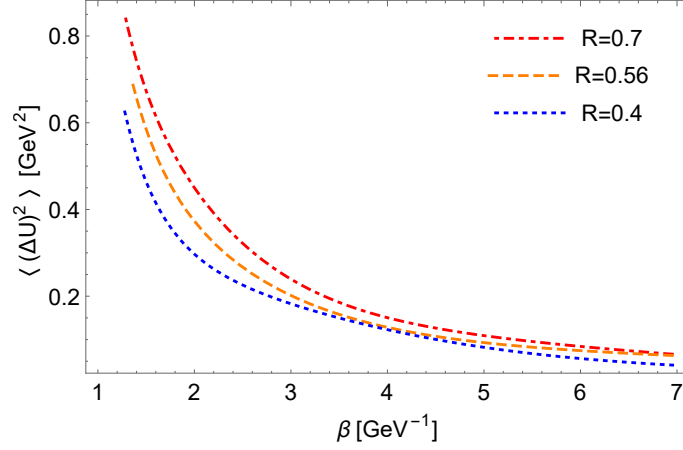


Figure 5: The variation of energy  $\langle (U(\beta))^2 \rangle$  as derived in Eq. (29) as a function of  $\beta$ . The parameters  $R$  and  $\alpha_s$  take the values 0.7, 0.56, 0.4 fm associated to  $0.66\pi, 0.2, 0.1$ , respectively.  $f_0(500)$  and charmonium values are denoted in red and orange colors.

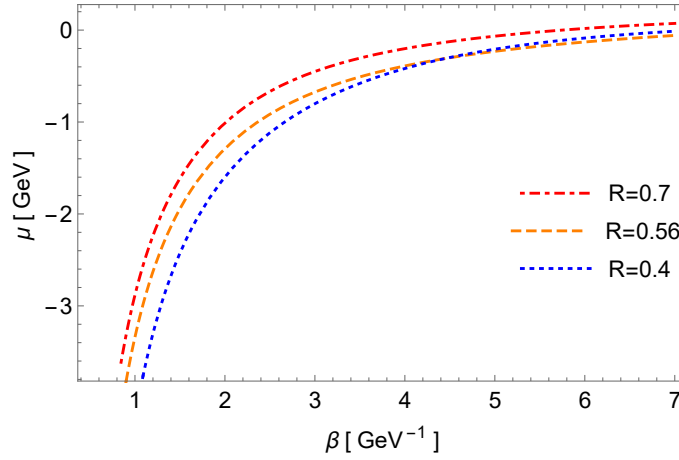


Figure 6: The chemical potential as derived in Eq. (35) as a function of  $\beta$ .  $f_0(500)$  and charmonium values are denoted in red and orange colors.

with

$$D = 36E_0^2 e^{-3\beta E_0} + \frac{15\sqrt{\pi} E_0^2 e^{\beta E_0}}{16 (\beta E_0)^{\frac{7}{2}}} - \frac{3\sqrt{\pi} E_0^2 e^{\beta E_0}}{4 (\beta E_0)^{\frac{5}{2}}} + \frac{\sqrt{\pi} E_0^2 e^{\beta E_0}}{4 (\beta E_0)^{\frac{3}{2}}} + \frac{1}{\gamma\beta^3}.$$

Finally, the heat capacity is obtained from Eq. (27) as:

$$\begin{aligned} C(\beta) &= \frac{\partial U(\beta)}{\partial T} = -K_B \beta^2 \frac{\partial U(\beta)}{\partial \beta} \\ &= K_B \beta^2 \left( \left( \frac{A}{B} \right)^2 - \frac{D}{B} \right). \end{aligned} \quad (30)$$

Also, we calculate Helmholtz's free energy  $F(\beta)$  [1] as:

$$F(\beta) = -K_B T \ln(Z(\beta)), \quad (31)$$

leading to

$$F(\beta) = -\frac{1}{\beta} \ln(B). \quad (32)$$

Then, from Eq. (31) the entropy,  $S(\beta)$ , is concluded [1] as,

$$S(\beta) = -\frac{\partial F(\beta)}{\partial T} = K_B \beta^2 \frac{\partial F(\beta)}{\partial \beta}, \quad (33)$$

yielding (after some algebraic manipulations) the following expressions,

$$S(\beta) = K_B \beta \left( \frac{A}{B} + \frac{\ln(B)}{\beta} \right) \quad (34)$$

Eventually, the chemical potential  $\mu(\beta)$  calculated [1] as,

$$\begin{aligned} \mu(\beta) &= -T \frac{\partial S(\beta)}{\partial N} = -\frac{1}{K_B \beta} \frac{\partial S(\beta)}{\partial N}, \\ &= -\frac{1}{N} \left( \frac{A}{B} + \frac{\ln(B)}{\beta} \right). \end{aligned} \quad (35)$$

It should be noticed that one has to consider two different cases, corresponding to high and low temperatures  $T$  and compare with  $T_{rot}$  which determines the temperature scale relevant to rotational degrees of freedom. Figures 4, 5, and 6 show these thermodynamical quantities as a function of  $\beta$ . All subsequent calculations have been performed for the parametrization of the potential given in Eq. (7).

Figure 7 shows the dependence of the chemical potential  $\mu$  on the temperature  $T$ , whereas Figure 8 shows the dependence of the chemical potential  $\mu$  on the volume  $V$ . The bump of positive  $\mu(T)$  values near origin appears as a typical artifact of using approximate methods in the evaluation of the thermodynamic properties of the Bose gas leading to expressions in closed form, an

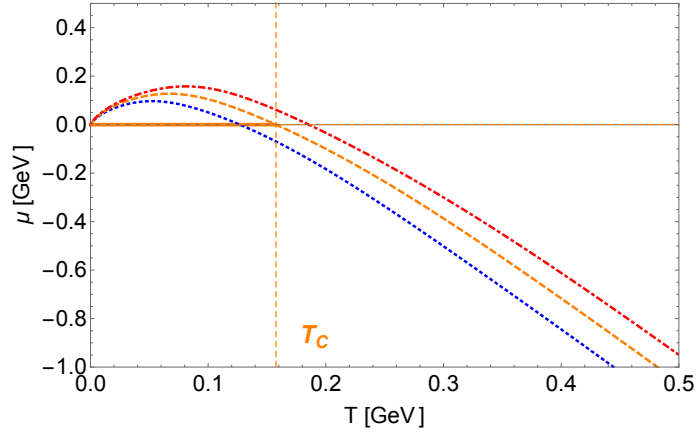


Figure 7: The chemical potential as derived in Eq. (35) as a function of temperature.  $f_0(500)$  and charmonium values are denoted in red and orange colors, see the text for discussion.

issue discussed in [25]. In reality, the  $\mu(T)$  curve has to follow the plateau of vanishing values from origin to the critical point (thick segment on the horizontal axis) at which it bends and starts falling downward. Within this context, more elaborate numerical calculations would be required in future studies in order to rise the precision of the predictions of the critical points at which the phase transition takes place.

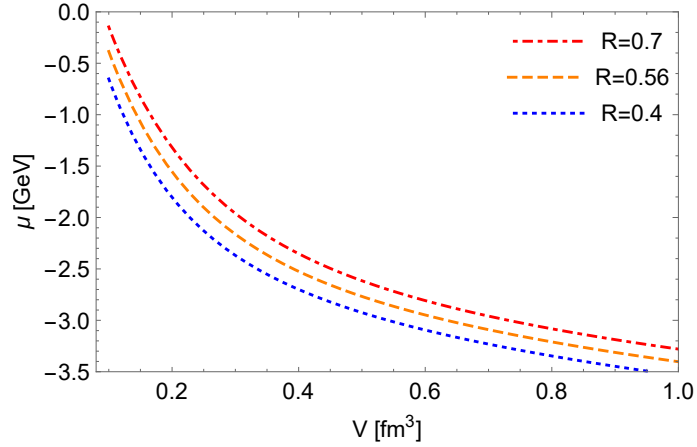


Figure 8: The chemical potential as derived in Eq. (35) as a function of volume.  $f_0(500)$  and charmonium values are denoted in red and orange colors.



### 3.1 Low temperature limit

The low temperature limit,

$$T_{rot} \gg T_c \gg T_0 = \frac{\hbar^2 c^2}{mR^2}, \quad (36)$$

equivalently,

$$1 \gg \frac{\hbar c}{mR}, \quad \text{or} \quad m \gg \frac{\hbar c}{R}, \quad (37)$$

where  $m$  is the mass of the particles in the gas, is of interest in thermal phenomena in QCD [26]. Indeed, for

$$R \ll \frac{\hbar c}{\Lambda_{QCD}}, \quad \Lambda_{QCD} \sim 200 \text{ MeV}, \quad (38)$$

with  $\Lambda_{QCD}$  denoting the QCD scale parameter, it corresponds to the weak coupling regime of QCD, in which a perturbative description of phase transitions is possible. According to the  $AdS_5/CFT_4$  gauge-gravity duality conjecture, such transitions appear dual to similar transitions in gravity, like the transitions of  $AdS$  spaces to  $AdS$  black holes. As a reminder, the  $S^1 \times S^3$  geometry emerges within this scheme as the conformal boundary (the null ray cone) of the  $AdS_5$  spacetime upon its conformal compactification.

In the case of low temperature, we may approximate the rotational partition function in Eq. (22) by

$$T \ll T_{rot} \rightarrow Z(\beta) \cong \frac{1}{2\gamma\beta} + 4e^{-3\beta E_0}. \quad (39)$$

The latter equation manifests the exponential decrease of the partition function with the increase of  $\beta$ . Then, the internal energy from Eqs. (26) and (39) calculates as:

$$T \ll T_{rot} \rightarrow U(\beta) = \frac{A}{B}, \quad (40)$$

with

$$\begin{aligned} A &= 12 E_0 e^{-3\beta E_0} + \frac{1}{2\gamma\beta^2}, \\ B &= 4 e^{-3\beta E_0} + \frac{1}{2\gamma\beta}. \end{aligned} \quad (41)$$

Moreover, from Eqs. (29) and (39) the variation of the energy (or "energy fluctuation") emerges as:

$$T \ll T_{rot} \rightarrow \langle (\Delta U(\beta))^2 \rangle = \left( \frac{A}{B} \right)^2 - \frac{D}{B}, \quad (42)$$

with

$$D = 36 E_0^2 e^{-3\beta E_0} + \frac{1}{\gamma\beta^3}. \quad (43)$$

In effect, the heat capacity  $C(\beta)$  is found as,

$$T \ll T_{rot} \rightarrow C(\beta) = -K_B \beta^2 \left( \left( \frac{A}{B} \right)^2 + \frac{D}{B} \right). \quad (44)$$

Finally, from Eqs. (31), (33) and (39), Helmholtz's free energy and the entropy are calculated as:

$$T \ll T_{rot} \rightarrow F(\beta) = -\frac{1}{\beta} \ln(B), \quad (45)$$

and

$$T \ll T_{rot} \rightarrow S(\beta) = K_B \beta \left( \frac{A}{B} + \frac{\ln(B)}{\beta} \right), \quad (46)$$

respectively. The low  $T$  condition in (36) is pretty well fulfilled by heavy flavor mesons, such as the charmonium, whose mass is  $m_{c\bar{c}} = 3097$  MeV. Indeed, for the corresponding hyperradius value of  $R = 0.56$  fm, used through the calculation, which has been fitted to the spectrum [27], the rotational temperature of  $T_{rot} = 352$  MeV is by about an order of magnitude larger than  $T_0 = 40$  MeV. This justifies hitting the Hagedorn's temperature as critical temperature for a Bose gas of such particles (vertical dashed line in Fig. 7).

As to the  $f_0$  meson gas, the inequality in (36) is fulfilled only for larger though not for much larger values between the involved quantities, which may explain why the related  $T_c$  still falls in the reasonable range of changes around Hagedorn's critical temperature of  $T_H = 0.16$  GeV (c.f. [28]).

### 3.2 High temperature limit

In the high temperature limit the partition function is calculated as,

$$T \gg T_{rot} \rightarrow Z(\beta) = \frac{\sqrt{\pi}}{4} \frac{1}{(E_0\beta)^{\frac{3}{2}}} e^{\beta E_0}. \quad (47)$$

Now, we turn our attention to the internal energy, given by

$$T \gg T_{rot} \rightarrow U(\beta) = \left( \frac{3}{2\beta} - E_0 \right) = K_B \left( \frac{3}{2}T - T_{rot} \right), \quad (48)$$

equivalently,

$$\begin{aligned} T \gg T_{rot} \rightarrow U(\beta) &= \frac{3}{2} K_B T \\ &= \frac{3}{2} \left( \frac{1}{\beta} \right). \end{aligned} \quad (49)$$

The heat capacity  $C(\beta)$  is evaluated as:

$$T \gg T_{rot} \rightarrow C(\beta) = \frac{3}{2} \left( \frac{1}{T\beta} \right) \quad (50)$$

Next we calculate the variation of the energy, Helmholtz's free energy, and the entropy as:

$$T \gg T_{rot} \rightarrow \langle (\Delta U(\beta))^2 \rangle = \frac{3}{2} (K_B T)^2 = \frac{3}{2} \left( \frac{1}{\beta} \right)^2, \quad (51)$$

and,

$$T \gg T_{rot} \rightarrow F(\beta) = -\frac{1}{\beta} \ln \left( \frac{\sqrt{\pi}}{4} (E_0 \beta)^{-\frac{3}{2}} \right) - E_0, \quad (52)$$

and,

$$T \gg T_{rot} \rightarrow S(\beta) = -K_B \left[ \frac{3}{2} + \ln \left( \frac{\sqrt{\pi}}{4} (E_0 \beta)^{-\frac{3}{2}} \right) \right]. \quad (53)$$

## 4 The grand canonical partition function $z(\beta, V, \mu)$ and related thermodynamic functions

The grand canonical partition function, here denoted by  $z(\beta, V, \mu)$  is related to the canonical partition function  $Z(\beta, R, b)$  for a system with N particles, as:

$$z(\beta, V, \mu) = \sum_{N=0}^{\infty} \frac{1}{N!} (e^{\beta\mu} Z(\beta, R, b))^N, \quad (54)$$

where  $\mu$  stands for the chemical potential energy. For non-interacting systems where particles are free to move and exchange positions (such as quantum gases), we know from the factorization theorem [29] that the Eq. (54) is reduced to:

$$z(\beta, V, \mu) = \frac{1}{(1 - e^{\beta\mu} Z(\beta, R, b))}, \quad (55)$$

where V is the "volume" (three dimensional hypersurface) of the system which is well known [13] and reads:

$$V = 2\pi^2 R^3, \quad (56)$$

implying,

$$R = \left( \frac{V}{2\pi^2} \right)^{1/3}. \quad (57)$$

As long as we need to study the canonical partition function  $Z(\beta, R, b)$  as a function of the volume, we have to express  $R$  in terms of  $V$ . We begin with Eq. (8) with the aim to find the volume dependence of the ground state energy  $E_0$ . In order to do that, some detailed instructions regarding the calculations are needed. We will continue taking as an illustrative example of a color-charge dipole gas the one constituted by  $f_0$  (500) mesons, in which case the parameters take the following values:  $\hbar c = 197.3289$  MeV fm,  $Mc^2 = 250$  MeV,  $N_c = 3$  and  $R = 0.7$  fm. For the case of  $f_0$  (500), the strong coupling constant takes the value of  $\alpha_s = 0.66\pi$  [13, 30]. Substitution of these values in Eq. (7), yields,

$$b = \frac{3 \times 0.66 \pi}{2}. \quad (58)$$

The above potential parameters have been shown to fit data on the  $f_0(500)$  meson excitation energies. Thus, substituting above values and Eqs. (57) and (58) in to Eq. (8), gives,

$$E_0 = \frac{1.8}{V^{2/3}}, \quad \gamma = \frac{0.56}{V^{2/3}} \text{ [GeV]}. \quad (59)$$

Hence, placing Eq. (59) in to Eq. (23),  $Z(\beta, V, b)$  becomes,

$$Z(\beta, V, b) = \frac{0.8 V^{2/3}}{\beta} + 4 e^{\left(\frac{-5.4 \beta}{V^{2/3}}\right)} + \frac{0.2 e^{\left(\frac{1.8 \beta}{V^{2/3}}\right)}}{\left(\frac{\beta}{V^{2/3}}\right)^{3/2}}. \quad (60)$$

Upon substitution of Eq. (60) into Eq. (54),  $z(\beta, V, \mu)$  emerges as,

$$z(\beta, V, \mu) = \frac{1}{1 - A},$$

$$A = e^{\beta\mu} \left( \frac{0.8 V^{2/3}}{\beta} + 4 e^{\left(\frac{-5.4 \beta}{V^{2/3}}\right)} + \frac{0.2 e^{\left(\frac{1.8 \beta}{V^{2/3}}\right)}}{\left(\frac{\beta}{V^{2/3}}\right)^{3/2}} \right). \quad (61)$$

Next we need to obtain the grand canonical potential [29] as,

$$\begin{aligned} \Omega(\beta, V, \mu) &= -K_B T \ln(z(\beta, V, \mu)) \\ &= \frac{1}{\beta} \ln(1 - A). \end{aligned} \quad (62)$$

From the latter equation, the particle number  $N$  can be determined as,

$$\begin{aligned} N &= - \left( \frac{\partial \Omega(\beta, V, \mu)}{\partial \mu} \right)_{\beta, V} \\ &= \frac{A}{1 - A}. \end{aligned} \quad (63)$$

Now one is ready to calculate the pressure  $P$  as,

$$\begin{aligned} P &= - \left( \frac{\partial \Omega(\beta, V, \mu)}{\partial V} \right)_{\beta, \mu} = \frac{B e^{\beta\mu}}{\beta(1 - A)}, \\ B &= \frac{0.56}{\beta V^{1/3}} + \frac{14 \beta e^{\left(\frac{-5.4 \beta}{V^{2/3}}\right)}}{V^{5/3}} + \frac{0.2 \beta e^{\left(\frac{1.8 \beta}{V^{2/3}}\right)}}{V^{5/3} \left(\frac{\beta}{V^{2/3}}\right)^{5/2}} - \frac{0.2 \beta e^{\left(\frac{1.8 \beta}{V^{2/3}}\right)}}{V^{5/3} \left(\frac{\beta}{V^{2/3}}\right)^{3/2}}. \end{aligned} \quad (64)$$

Finally, we are interested to study the dependence of the pressure on the strong coupling  $\alpha_s$  and evaluate  $P$  for the case of the charmonium for which we adopt the  $\alpha_s = 0.2$  value, and set  $Mc^2 = 750$  MeV as in [30, 27]. In so doing, the equation (8) yields

$$b = \frac{3 \times 0.2}{2}. \quad (65)$$

Substitution of this value into Eq.(8), yields

$$E_0 = \frac{7.09}{V^{2/3}}, \quad \gamma = \frac{0.2}{V^{2/3}} \text{ [GeV]}. \quad (66)$$

Hence, inserting Eq. (60) into Eq. (41) allows us to write  $Z(\beta, V, b)$  as,

$$Z(\beta, V, b) = \frac{2.6 V^{2/3}}{\beta} + 4 e^{\left(\frac{-21 \beta}{V^{2/3}}\right)} + \frac{0.02 e^{\left(\frac{7.09 \beta}{V^{2/3}}\right)}}{\left(\frac{\beta}{V^{2/3}}\right)^{3/2}}. \quad (67)$$

Now substitution of Eq. (67) into Eq. (55) leads to

$$z(\beta, V, \mu) = \frac{1}{1 - A},$$

$$A = e^{\beta\mu} \left( \frac{2.6 V^{2/3}}{\beta} + 4e^{\left(\frac{-21 \beta}{V^{2/3}}\right)} + \frac{0.02 e^{\left(\frac{7.09 \beta}{V^{2/3}}\right)}}{\left(\frac{\beta}{V^{2/3}}\right)^{3/2}} \right). \quad (68)$$

With that, the grand canonical potential  $\Omega$  calculates as,

$$\Omega(\beta, V, \mu) = \frac{1}{\beta} \ln(1 - A). \quad (69)$$

and allows to express the number of particles  $N$  according to,

$$N = \frac{A}{1 - A}. \quad (70)$$

In effect, the pressure  $P$  takes the form of,

$$P = -\frac{e^{\beta\mu} F}{\beta D}, \quad (71)$$

with

$$F = \frac{1.75}{\beta V^{1/3}} + \frac{56 \beta e^{\left(\frac{-21 \beta}{V^{2/3}}\right)}}{V^{5/3}} + \frac{0.02 \beta e^{\left(\frac{7.09 \beta}{V^{2/3}}\right)}}{V^{5/3} \left(\frac{\beta}{V^{2/3}}\right)^{5/2}} - \frac{0.11 \beta e^{\left(\frac{7.09 \beta}{V^{2/3}}\right)}}{V^{5/3} \left(\frac{\beta}{V^{2/3}}\right)^{3/2}},$$

$$D = \beta (1 - H e^{\beta\mu}),$$

$$H = \left( \frac{2.6 V^{2/3}}{\beta} + 4 e^{\left(\frac{-21 \beta}{V^{2/3}}\right)} + \frac{0.02 e^{\left(\frac{7.09 \beta}{V^{2/3}}\right)}}{\left(\frac{\beta}{V^{2/3}}\right)^{3/2}} \right).$$

The pressure as a function of the chemical potential is plotted in the Figs. 9 and 10, where the parameter  $\beta$  takes the value of 4 GeV<sup>-1</sup>. Compared to the pressure in the  $f_0(500)$  meson gas (shown in Fig. 9) the pressure for the charmonium (illustrated by Fig. 10) presents itself significantly higher. This means that the charmonium gases are more compact than  $f_0(500)$  meson systems, as it should be.

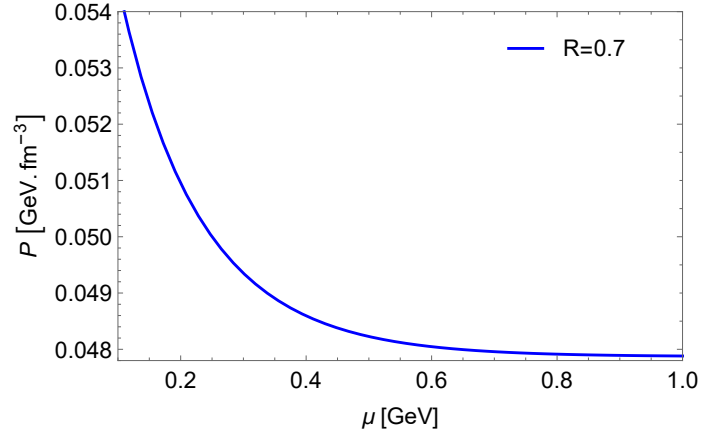


Figure 9: The pressure as derived in Eq. (64) as a function of  $\mu$  for the  $f_0(500)$  mesons. The parameters  $R$  and  $\alpha_s$  take the value 0.7 fm and  $0.66 \pi$ , respectively.

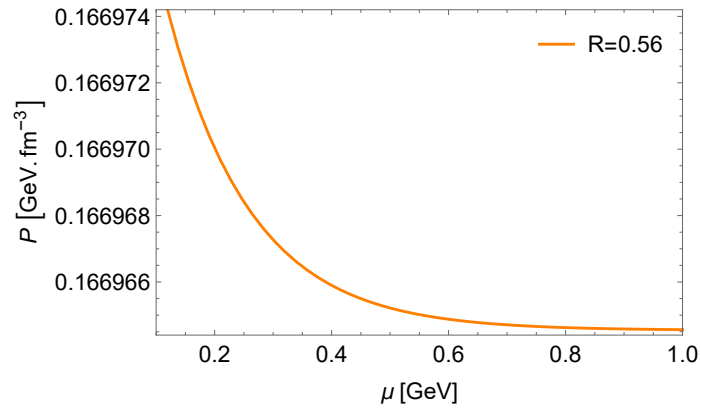


Figure 10: The pressure as derived in Eq. (71) as a function of  $\mu$  for the charmonium. The parameters  $R$  and  $\alpha_s$  take the value 0.56 fm and 0.2, respectively.

## 5 Summary and Conclusions

In this work we studied the thermodynamic properties of the trigonometric Rosen-Morse potential in the parametrization of Eqs. (3) and (7), and from the perspective of its utility as an effective potential in color-neutral quark systems. The parametrization chosen allowed to cast the one-dimensional Schrödinger potential problem as a perturbation of free quantum motion on the three-dimensional hyper-sphere,  $S^3$ , a manifold of finite volume that can host only charge-neutral systems, such as color-charge neutral mesons. It has to be noticed that preferring the hyper-sphere is not essential for the modelling of the charge-neutrality because any manifold without boundary, be it symmetric or not, can bear only charge-neutral systems. The  $S^3$  manifold brings the advantage of a particularly simple form of the Laplace-Beltrami operator that gives rise to an exactly solvable dynamics and degeneracy patterns in the excited levels of the type observed in some light mesons, such as  $f_0$  and  $a_0$  [13]. The potential under discussion has found applications besides in the sector of the light unflavored mesons [13], also in heavy quarkonia [27]. In both cases it has been found to provide quite a realistic data description. Therefore, the canonical and grand canonical partition functions calculated here account for

- color electric charge neutrality,
- multiplicities of states in the levels,
- finite volumes.

Accounting for the state multiplicity effects, caused an increase in the values of the Canonical partition function. A similar consequence is observed due to the shrinkage of the volume of the system though this effect is not that significant in magnitude as the presence of degeneracy. Our results were illustrated for the case of the charmonium and the  $f_0(500)$  meson. In particular we observed that a charmonium gas is more compact as the one constituted by  $f_0(500)$  mesons, as is to be expected. From Fig. 7 we read off quite reasonable values of the critical temperature as  $T_c \in [0.157 - 0.175]$  GeV, a range of variations around Hagedorn's value also quoted by other authors [28].

To the amount the majority of the mesons detected so far are commonly accepted to be color-anti-color (quark-anti-quark) dipoles, a picture also adaptable to baryons when considered as quark-diquark configurations, therefore we expect the finding of the present study to be useful to studies of thermodynamic aspects of QCD phenomena [31]. The advantage of the method presented here is that in being based on fundamental color dipoles, it allows, by the aid of the techniques known from the physics of diatomic molecules, to track down phase transitions from gaseous to liquid states of colorless quark matter and considering the dipole dissociation [32] towards colored states.

Furthermore, this approach allows to control the state of matter through the topology of the internal space [33] of hadrons whose running curvature could be made temperature dependent and allowed to vary between positive

and negative values. The latter case would not prohibit observability of single charges and is expected to provide a scenario toward color deconfinement. Consequently, this manuscript provides the necessary building blocks required by future phase transition studies [34] within a quantum mechanical approach to QCD, which manifestly takes into account the fundamental field theoretical concept of colorlessness of hadrons and which in addition explicitly depends on the strong coupling constant and the number of colors.

All in all, we have worked out the canonical and grand canonical partition functions related to the trigonometric Rosen-Morse potential together with the principal thermodynamic functions and consider them as promising tools for an adequate description of color neutral states of hadronic matter as they appear in heavy-ion collisions and applications to matter in compact stars, a topic for future research.

## 6 Acknowledgements

We thank David Blaschke for inspiring discussions on the aspects of quark confinement. D. A-C. acknowledges support from the the Bogoliubov-Infeld program for collaboration between JINR and Polish Institutions as well as from the COST actions CA15213 (THOR) and CA16214 (PHAROS).

## References

- [1] W. G. Hoover, *Computational statistical mechanics*, Elsevier (2012)
- [2] R. Baron, D. Trzesniak, A. H. de Vries, A. Elsener, S. J. Marrink, W. F. van Gunsteren. *ChemPhysChem* **8**(3), 452-461 (2007)
- [3] A. N. Ikot, E. O. Chukwuocha, M. C. Onyeaju, C. A. Onate, B. I. Ita, M. E. Udoh, *Pramana*, **90**(2), 22 (2018)
- [4] A. Hashemloo, C. M. Dion, *The Journal of chemical physics*, **143**(20), 204308 (2015)
- [5] K. S. Drellishak, D. P. Aeschliman, A. B. Cambel, *The Physics of Fluids*, **8**(9), 1590-1600 (1965)
- [6] B.N. Partiw, A. Suprami, C. Cari, A.S. Husein, *Pramana-J.Phys.* **88**(25) (2017)
- [7] C.O. Edet, P.O. Amadi, A.N. Ikot, U.S. Okorie, A. Tas, G. Rampho, E-Print arXiv: 1912.00148[quant-physics] <https://arxiv.org/abs/1912.00148>
- [8] F. Cooper, A. Khare, U. Sukhatme, *Phys. Rept.* **251**, 267-385 (1995)
- [9] E. G. Kalnins, W. Miller, Jr., G. S. Pogosyan, *Phys. Atom. Nucl.* **65**, 1086-1094 (2002)



- [10] L. D. Landau, E. M. Lifschits, *The Classical Theory of Fields*, Pergamon Press. p. 335 (1971)
- [11] S. R. Valluri, M. Gil, D. J. Jeffrey, and Sh. Basu, *J. Math. Phys.* **50**, 102103 (2009)
- [12] S. M. Blinder, *Journal of Mathematical Chemistry*, **19**(1), 43-46 (1996)
- [13] M. Kirchbach, C. B. Compean, *Eur. Phys. J. A* **52**(7), 210 (2016). Addendum: [*Eur. Phys. J. A* **53**(4), 65 (2017)]
- [14] S. S. Afonin, *Int. J. Mod. Phys. A* **23**, 4205 (2008)
- [15] C. B. Compean, M. Kirchbach, *J. Phys. A* **39**, 547 (2006)
- [16] A. P. Raposo, H. J. Weber, D. E. Alvarez-Castillo and M. Kirchbach, *Central Eur. J. Phys.* **5**(3), 253-284 (2007)
- [17] M. Abu-Shady, S. Y. Ezz-Alarab, *Few Body Syst.* **60**(4), 66 (2019)
- [18] C. Cook and R. H. Dickerson, *American Journal of Physics* **63**, 737 (1995)
- [19] V. V. Begun and M. I. Gorenstein, *Phys. Lett. B* **653**, 190-195 (2007)
- [20] G. B. Arfken, H. J. Weber, F. E. Harris, *Mathematical Methods for Physicists, 7th edition*, Waltham, MA, Elsevier (2013)
- [21] S. Wen, *Introduction to Numerical Computation*, World Scientific (2019)
- [22] D. Ebert, R. N. Faustov, V. O. Galkin, *Phys. Rev. D* **67**, 014027 (2003)
- [23] T. Das, *EJTP* **13**, 207 (2016)
- [24] W.A. Yahya, K.J. Oyewumi. *Assoc. Arab. Univ. Basic Appl. Sci.* **21**(53) (2016)
- [25] A. G. Sotnikov, K. V. Sereda, Yu.V. Slysarenko, *Low Temperature Physics*, **43**, 144-152 (2017)
- [26] S. Hands, T. J. Hollowood, and J. C. Myers, *JHEP* **1007**, 086 (2010)
- [27] A. Al-Jamel, *Mod. Phys. Lett. A* **34**(37), 1950307 (2019)
- [28] L. Maiani, F. Piccinini, A. D. Poloso, and V. Riquer, *Nucl. Phys. A* **748**, 209-225 (2005)
- [29] Reif, F., *Fundamentals of statistical and thermal physics*, Waveland Press (2009)
- [30] M. Tanabashi *et al.* [Particle Data Group], *Phys. Rev. D* **98**, no.3, 030001 (2018)
- [31] A. Ayala, M. Martinez, G. Paic, G. T. Sanchez, *Phys. Rev. C* **77**, 044901 (2008)

- [32] A. Dubinin, D. Blaschke and Y. L. Kalinovsky, *Acta Phys. Polon. Supp.* **7**, no.1, 215-223 (2014)
- [33] L. Casetti, M. Pettini and E. G. D. Cohen, *Phys. Rept.* **337**, 238-341 (2000)
- [34] J. B. Elliott and A. S. Hirsch, *Phys. Rev. C* **61**, 054605 (2000)